



DOI: 10.22144/ctu.jen.2023.016

Enhancement of photocatalytic activity of TiO₂ for gaseous toluene removal by simple mechanical mixing with modified zeolite

Thai Le Truong Giang¹, Quang Thi Hue Minh¹, Thai Nguyen Trieu Nguyen¹, Cu Hoang Minh¹, Le Ky Anh¹, Mai Hai Nghi¹, Le Huy Hoang¹, Nguyen Quang Long^{1,2*}, and Ngo Tran Hoang Duong^{1,2}

¹Faculty of Chemical Engineering, Ho Chi Minh City University of Technology, Viet Nam

²Vietnam National University Ho Chi Minh City, Viet Nam

*Correspondence: Nguyen Quang Long (email: nqlong@hcmut.edu.vn)

Article info.

Received 13 Nov 2022

Revised 05 Dec 2022

Accepted 08 Dec 2022

Keywords

Mesoporous zeolite,
Photocatalyst, TiO₂, Toluene,
Microwave-assisted method

ABSTRACT

A zeolite Y was modified by the microwave-assisted method (MWA) for generating mesopores and was mechanically mixed with TiO₂ for photocatalytic application. The external surface area, which is represented to the mesopore, was significantly increased about 5 to 10 times in the modified zeolites compared to the parent zeolite. The catalysts were used to catalyze the gas phase photodegradation of toluene, a volatile organic compound (VOC). The photocatalytic activity and stability of the catalyst were improved when the mesoporous zeolite was presented. The mechanical mixture contained 30 wt%. TiO₂ and 70 wt%. mesoporous zeolite showed the highest toluene removal efficiency.

1. INTRODUCTION

VOCs, or volatile organic compounds, are carbon-based organic chemicals that come from solids or liquids and can vaporize at room temperature (Kamal et al., 2016). Although VOCs may or may not be toxic, they typically refer to volatile toxic organic compounds in industrial production such as solvents toluene, formaldehyde, benzene, acetone, ethanol, trichloroethane (TCE) (Huang et al., 2014; Bari et al., 2018). When mixed in the air, various types of VOCs can bond or react with other gaseous molecules to form new compounds. VOCs come from a variety of emission sources, many of which are released directly into the air with no treatment. For example, car exhaust, gasoline-powered lawn and garden equipment, household chemicals, etc. Figure 1 shows how VOC emissions in New England, USA, were distributed among various sectors in 2011. The emission sources of VOC came mainly from solvent and non-road mobile, which accounted for more than half of VOC emissions during 2011.

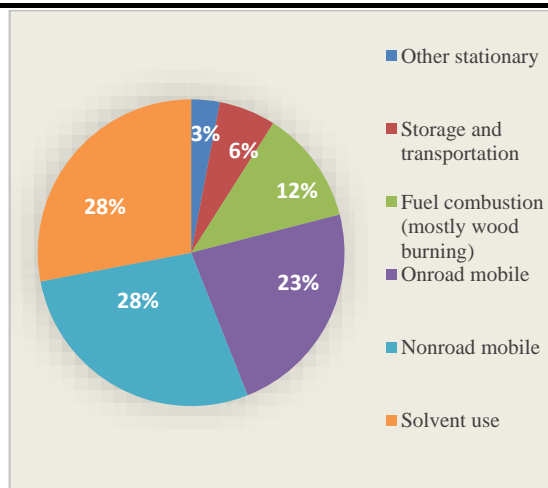
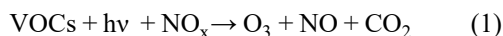


Figure 1. An example of VOC Emissions

(Source: EPA, n.d.)

VOCs in gas streams are potential pollutants because of their strong odor and toxicity. With the human body, VOCs can cause eye and throat

irritation, liver damage, central nervous system damage, etc. Long-term exposure can lead to cancer (Bari et al., 2018; Molhave et al., 1991). Moreover, VOCs are one factor that generates ozone, an air pollutant. VOCs react with NO_x in sunlight, creating low-energy ozone, which combines with fine dust to form fog. It is worth mentioning that the CO_2 released from the above process is the cause of the greenhouse effect and global warming (Berezina et al., 2020):



In reality, a variety of photocatalytic materials, including binary compounds: copper (II) oxide, iron (III) chloride, iron (III) oxide, titanium (IV) oxide, ternary compounds such as tungstates, bismuthates, vanadates, and complex oxyhalides have been used as catalysts for the treatment of toluene – a typical volatile organic compound (Talaiekhosani et al., 2021). TiO_2 is the most commonly used photocatalyst in air purification (Binas et al., 2017). The TiO_2 /adsorbent composites have been intensively investigated. Many materials have been used to support the deposition of TiO_2 , such as activated carbon (Mombello et al., 2009), silica materials (Kutluay et al., 2020), alumina (Li et al., 2019). The composite photocatalyst/adsorbent system is more beneficial compared to the separate application of photocatalyst and adsorbent because of the reversible transfer of intermediates and receiving species between the two photocatalyst and adsorbent surfaces (Kovalevskiy et al., 2018). Zeolites are one of the most potential adsorbents

because of their high cation-exchange capacities and surface areas. Following the treatment by microwave-assisted chelation (MWAC), a zeolite remarkably improves the area and volume of mesopores. The mesoporous zeolites can enhance the efficiency of the reversible transfer intermediates and receiving species between TiO_2 and the zeolite.

Based on positive results from pioneering works, this study aims to develop another novel photocatalytic composite, namely TiO_2 -mesoporous zeolitic material type Y (TiO_2 -mesoY). Mesoporous zeolite Y was synthesized by employing MWAC on a commercial Y zeolite using a commercial microwave instead of a specialized microwave reactor, followed by incorporating TiO_2 via ion exchange. The material characterizations and the application as catalysts for the photodegradation of toluene were reported and discussed.

The mechanism of photocatalytic removal of toluene from the air was described by Mamaghani et al. (2017) as follows:

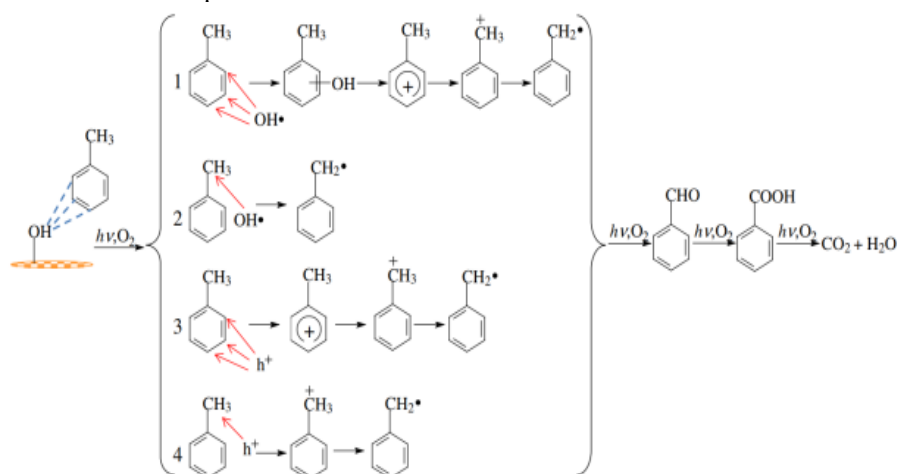
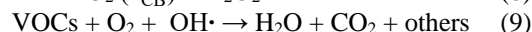
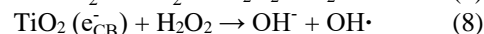
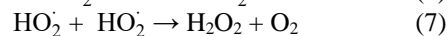
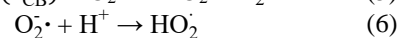
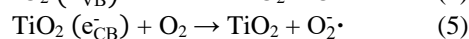
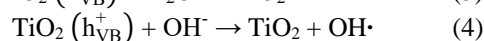
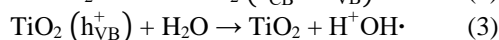
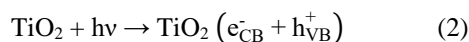


Figure 2. Proposed reaction route for the photocatalytic degradation of toluene on TiO_2

(Source: Zhang et al., 2014)

The formation of intermediate compounds is shown in Figure 2. Surface hydroxyls formed by water vapor interacting with TiO₂ surface can easily affect the adsorption and reaction processes. It was speculated that the weak-bonding between the surface hydroxyl group and the aromatic ring of toluene adsorbed on TiO₂ was suggested to be the OH... π -electron-type interaction. Therefore, the surface hydroxyl groups acting as active sites for toluene adsorption were introduced to enhance toluene adsorption on TiO₂ surface (Zhang et al., 2014). The end products of complete photocatalytic oxidation processes are carbon dioxide and water.

2. MATERIALS AND METHODS

In this study, catalysts for photocatalytic removal of gaseous toluene contained TiO₂ and zeolite or mesoporous zeolite. Commercial TiO₂ (P25) was purchased from Acros. Zeolite (Y type) in this study was synthesized according to our previous study (Tu et al., 2019) using liquid glass as the silica source, and denoted as M0. In order to form mesopore in the zeolite Y, sodium hydroxide, ethylenediaminetetraacetic acid (EDTA), ammonium chloride were all purchased from Xilong Co., and used without purification. The microwave-assisted method (MWA) for treatment of zeolite Y was performed using a commercial Electrolux microwave oven. To prepare the mixture, 5 g of zeolite Y was first added into 75 mL EDTA aqueous solution 0.2 M in a 500 mL glass reagent bottle under stirring for 5 minutes. The bottle containing the mixture was then inserted into the microwave for 20 minutes (sample M20) or 60 minutes (sample M60) at a power of 290 W. Next, the mixture was quenched using an ice bath for 10 minutes. Then, the sample was washed using 100 mL of NaOH 0.3 M aqueous solution for 10 minutes under stirring to remove the excess EDTA and the detrital material that remained in the zeolite pores. Finally, the sample was washed thoroughly using deionized water and dried at 80°C overnight. H-type zeolites were obtained by ion-exchanging with NH₄Cl at 60 °C for 1.5 hours, then be calcined at 400 °C for 3 hours. For the characterization of catalysts, the crystalline structure and composition were studied via XRD (D8 ADVANCE) using CuK α radiation (1.5406 Å) at 40 kV and 25 mA. XRD patterns were collected in the 2 θ range of 5°-50°. The nitrogen adsorption/desorption helped investigate surface areas and pore volume, using a Quantachrome NOVA 2200E surface area analyzer.

For measurement of the removal of toluene by photocatalysis process, the studied samples were initially converted to H-form. HY sample and other mesoporous zeolites M(x) were mechanically mixed with TiO₂, denoted as TiO₂-M(x). The zeolite and TiO₂ were mixed and dispersed in ethanol at a concentration of 0.1 g/mL and ultra-sonication for 10 minutes. The mixture is coated on the surface of the inner tube of the annular photocatalytic reactor by spray coating method and coated on the outer of quartz tube with 4 UV lamp (Sankyo Denki F10T8BLBs, $\lambda = 315 - 400$ nm, 1.5 W UV) was then turned on to measure the photocatalytic activity. For the photocatalytic test, a gas mixture of toluene, oxygen, and water vapor, and nitrogen was introduced into the annular reactor. The toluene and water vapor in the stream was generated by a bubbling method. In this report, by controlling the mass-controllers and the liquid-bath's temperatures, the oxygen concentration was fixed at 20 vol.%, while the water vapor concentration, toluene concentration can be varied in order to investigate the effect of these concentrations. In this study, total flow-rate of 50 mL/min, toluene concentration of 314 ppmv and 60% humidity were fixed. Adsorption percentage at *i* (minute) was calculated by the areas of the peaks:

$$\text{Adsorption (\%)} = \left(1 - \frac{A_i}{A_o}\right) \cdot 100\% \quad (10)$$

where A_o and A_i are the areas of the peaks at the beginning of the reaction and after *i* minutes, respectively, Adsorption (%) – adsorption percentage at *i* minute, %.

The toluene removal ψ_i was calculated from the equation:

$$\Psi_i = \frac{P_k F}{RT_k} \times \frac{1000}{m_{\text{TiO}_2}} \times \left(1 - \frac{A_i}{A_o}\right) \quad (\text{mmol} \cdot \text{g}^{-1} \cdot \text{h}^{-1}) \quad (11)$$

where P_k and T_k stand for the saturation pressure (atm) and temperature (K) of toluene, F is the inlet gas flow rate (L/h), R is the gas constant (L.atm.K⁻¹.mol⁻¹), m_{TiO_2} stands for the mass of TiO₂ in the catalyst (g), A_o and A_i are the areas of the peaks at the beginning of the reaction and after *i* minutes, respectively.

3. RESULTS AND DISCUSSION

3.1. Characterization of the catalysts

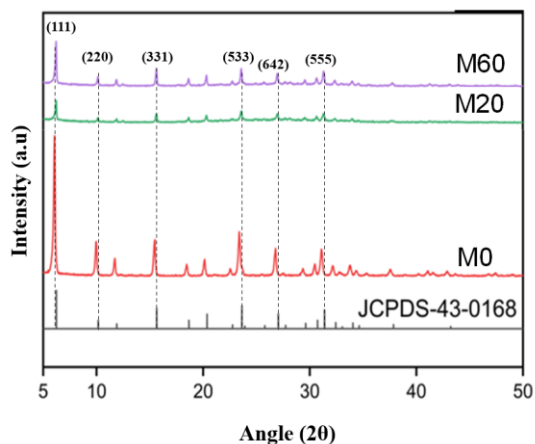


Figure 3. XRD patterns of the zeolites

Figure 3 shows the XRD patterns of the parent zeolite Y (M0) and the mesoporous zeolites Y (M20, M60), prepared by the MWA method. The diffraction result of these three mesoporous zeolitic materials was compared to the JCPDS standard of zeolite Y, showing that the prepared mesoporous zeolites retained the structure of the original zeolite. The characteristic diffraction peaks of mesoporous zeolite become less intense as the degree of denaturation increases. However, sample M60's peaks are higher than those of sample M20. This may be because a sufficiently long time of synthesis

provides Si atoms with a higher chance to shift to stabilize the structure. For M20, the smallest peaks reflect its greatly reduced crystallinity regarding M60 and the original M0.

Table 1 reports the surface area and pore volume of the three zeolites. It is seen that the surface areas of the generated mesoporous zeolite are lower than that of the parent zeolite Y, showing that a portion of the material has been washed away to form larger pores. The areas of mesopores of samples M20 and M60 increased significantly regarding that of M0. It is noteworthy that M60 has experienced a decrease in mesopores and an increase in micropores compared to M20. Table 1 also shows that the total pore volume hardly changes after the mesoporous modification process. Sample M60 has a larger micropore/mesopore volume than those of M20. The cause can be understood similarly to the above explanations how the long synthesis time affects the formation of new micropores. The topographical features of M0 and M60 are depicted through SEM images in Figure 4. The particles of the parent zeolite Y are relatively uniform in size and shape (Figures 4a and 4b). Meanwhile, a remarkable diversity is observed in the size of M60 particles (Figures 4c and 4d), and these particles also tended to clump together into larger clusters. This can be explained by the sudden increase in surface free energy when the pores are expanded. As a result, adjacent small particles have aggregated to reduce the surface area.

Table 1. Pore properties of sample

Sample	Specific pore volumes (cm ³ /g)			Specific surface areas (m ² /g)		
	V ^a _{total}	V ^b _{micro}	V ^c _{meso}	S _{BET}	S _{micropore}	S _{external (mesopore)}
M0	0.394	0.375	0.019	939	918	21
M20	0.278	0.082	0.196	395	192	203
M60	0.359	0.119	0.240	417	293	124

V_{total} : Total pore volume; V_{micro} : Micropore volume; V_{meso} : Mesopore volume;

^aTotal volume adsorbed at $p/p_0 = 0.99$, ^bBased on the t -plot method, ^c $V_{meso} = V_{total} - V_{micro}$

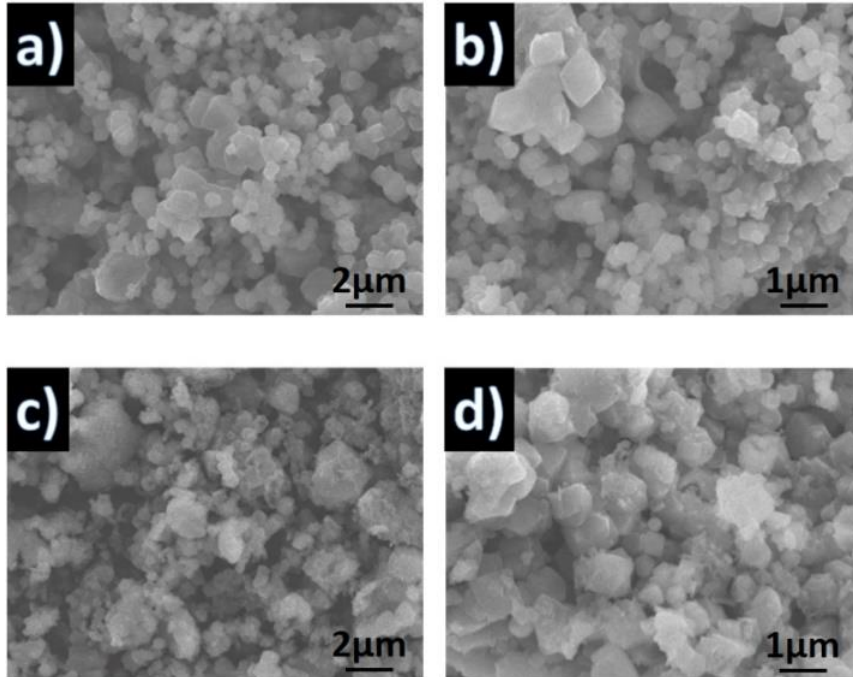


Figure 4. SEM images of (a, b) M0, (c, d) M60

3.2. Photocatalytic removal of toluene

3.2.1. Adsorption capacity

Figure 5 shows the percentage of adsorption of $\text{TiO}_2\text{-M}(x)$ samples over time. The detail toluene adsorption data are shown in Table 2. According to Figure 5, the shortest time to saturate the surface of TiO_2 was approximately 40 minutes. Such time increased remarkably when TiO_2 was mixed with $\text{M}(x)$. It took approximately 60 minutes for the microporous $\text{TiO}_2\text{-M0}$ to reach adsorption saturation. The respective values for mesoporous composites $\text{TiO}_2\text{-M20}$ and $\text{TiO}_2\text{-M60}$ were 90 and 120 minutes. The extended saturation adsorption time of $\text{TiO}_2\text{-M}(x)$ samples regarding P25 is ascribed to the presence of mesopores. According to Table 1, despite having the greatest microporous area, $\text{TiO}_2\text{-M0}$ only contains a moderate mesoporous area which is 6 - 10 times smaller than those of $\text{TiO}_2\text{-M20}$ and $\text{TiO}_2\text{-M60}$. The saturation adsorption time of $\text{TiO}_2\text{-M0}$ was therefore the shortest among $\text{TiO}_2\text{-M}(x)$ samples. Although $\text{TiO}_2\text{-M60}$ has fewer mesopores than $\text{TiO}_2\text{-M20}$ ($124 \text{ m}^2/\text{g}$ compared to $203 \text{ m}^2/\text{g}$), the former sample exhibited

a longer saturation adsorption time with toluene because of greater mesopore volume ($0.240 \text{ cm}^3/\text{g}$ compared to $0.196 \text{ cm}^3/\text{g}$).

Table 2 shows the detailed toluene adsorption data of pure TiO_2 and three $\text{TiO}_2\text{-M}(x)$ samples in high humidity and dynamic condition. In order to understand the role of TiO_2 and the modified zeolite on toluene adsorption in high humid condition, the amount of adsorbed toluene was measured on three criteria: by one gram sample, by the amount of TiO_2 in the sample, and surface area. Basing on the toluene concentration of the inlet/outlet stream and the flow-rate of the gas stream, the adsorbed toluene ($\mu\text{mol}/\text{g}$) was calculated from the mass balance during the adsorption experiments:

$$N_{\text{ADS_TOL}} = \frac{N_{\text{INLET_TOL}} - N_{\text{OUT_TOL}}}{m_{\text{SAMPLE}}} \quad (12)$$

After that, from the percentage of TiO_2 contains (%) in each sample and the specific surface area of each sample, the adsorbed toluene in other units ($\mu\text{mol}/\text{g}_{\text{TiO}_2}$, $\mu\text{mol}/\text{m}^2$) was obtained

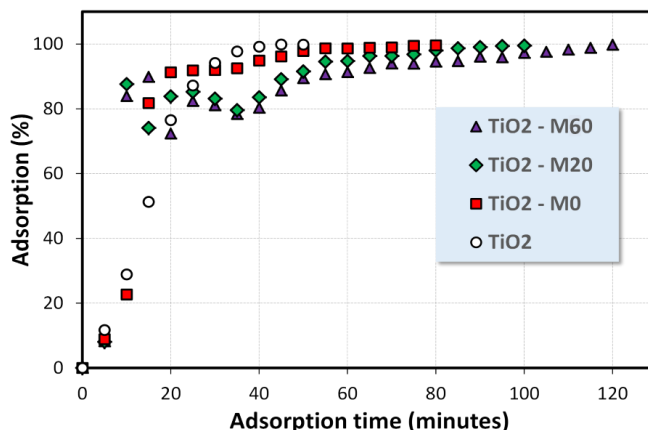


Figure 5. Relative toluene adsorption capacities of TiO₂ and TiO₂-M(x) samples (mixing mass ratio 3:7)

Table 2. Toluene adsorption of samples in high humidity and dynamic condition^a

Sample	TiO ₂ content(m%)	Amount of adsorbed toluene		
		μmol/g	μmol/g _{TiO₂}	μmol/m ² (^b)
TiO ₂	100	48.41	48.41	0.95
TiO ₂ -M0	30	45.56	151.88	0.07
TiO ₂ -M20	30	49.51	165.03	0.17
TiO ₂ -M60	30	57.82	192.74	0.19

^aAdsorption conditions: *F*=50 mL/min, *m_{cat}*= 0.2 g, *C_{Tol}* = 314 ppmv, relative humidity 60% at room temperature,

^bAssume: *S_{BET}*(mixture)= *S_{BET}*(TiO₂)*0.3 + *S_{BET}*(zeolite)*0.7

3.2.2. Effect of zeolite on the photocatalytic performance of TiO₂

Figure 6 compares the catalytic performance of P25-M(x) samples on the treatment of toluene after 20, 40 and 60 minutes. The results show that all catalyst samples, TiO₂ and TiO₂-M(x) composites, exhibited high levels of performance in the first 20 minutes, then experienced losses in activity. After 1 hour, the toluene conversion by TiO₂ was only 0.022 mmol⁻¹.g⁻¹.TiO₂.h⁻¹, while those of TiO₂-M0, TiO₂-M20, and TiO₂-M60 were 0.101, 0.148 and 0.205 mmol⁻¹.g⁻¹.TiO₂.h⁻¹ respectively. Based on these values, the order of catalytic durability can be inferred as TiO₂ < TiO₂-M0 < TiO₂-M20 < TiO₂-M60. The series shows the role of mesopores in improving the photodegradation performance and alleviating the deactivation of TiO₂-zeolite composites. The excellent adsorption capacity of a mesoporous material plays an essential role in capturing and decomposing toluene. Also, a large pore size facilitates the diffusion of reaction intermediates and thus limits the poisoning or blockage of active sites. As results from Figure 6 show the best efficiency and durability of the TiO₂-M60 catalyst, it will be used later to investigate different mixing ratios.

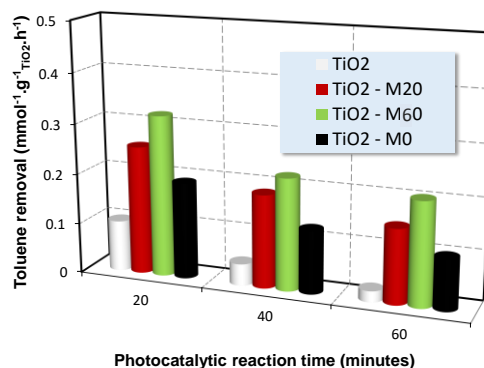


Figure 6. Catalytic performances of P25-M(x) samples (mixing mass ratio 3:7) on the photodegradation of toluene

3.2.3. Effect of mixing mass ratios on the photocatalytic performance of TiO₂

Figure 7 shows the influence of the mixing ratio between TiO₂ and M60 on the conversion of toluene. As percent of zeolite Y was increased from 0% (in TiO₂-M60 10:0) to 70% (in TiO₂-M60 3:7), the photocatalytic performance of the catalyst was significantly improved. At the 60th minute, for example, the toluene conversion rate of TiO₂ was only 0.022 mmol⁻¹.g⁻¹.TiO₂.h⁻¹, compared to 0.088

$\text{mmol}^{-1} \cdot \text{g}^{-1} \cdot \text{TiO}_2 \cdot \text{h}^{-1}$ of P25-M60 5:5 and $0.205 \text{ mmol}^{-1} \cdot \text{g}^{-1} \cdot \text{TiO}_2 \cdot \text{h}^{-1}$ of TiO_2 -M60 3:7. This rise in toluene conversion may be because of the ability to adsorb toluene of zeolite Y, leading to higher amount of toluene adsorbed when the amount of this material was increased. A similar tendency has been reported in (Tu et al., 2019) in which the enhancement of nano-sized Me/ TiO_2 with zeolite Y as an adsorbent (Me = Au, Pd) also showed an effective photocatalytic activity and stability for toluene photocatalytic oxidation in a continuous annular reactor under humid conditions. Another zeolite such as ZSM-5 also can help TiO_2 to improve the photocatalytic activity for toluene removal, as mentioned in (Dinh et al., 2018). Takeuchi also reported the positive effect of zeolite Y for toluene photocatalytic removal. By using ultra-stable Y zeolites (USY) as supports for TiO_2 , the TiO_2 /USY showed the highest reactivity for the photocatalytic oxidation of toluene and benzene (Takeuchi et al., 2012). The Y-zeolites adsorbed large amounts of toluene, condensed toluene in their hydrophobic cavities, and efficiently supplied them onto the TiO_2 photocatalyst surface.

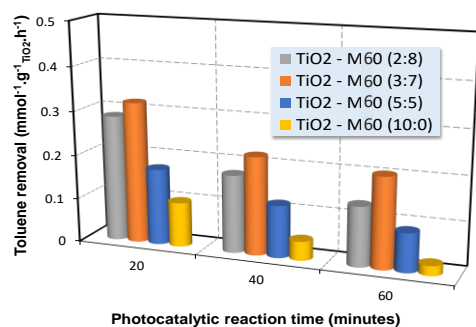


Figure 7. Catalytic performances of TiO_2 -M60 samples with different mixing mass ratios on the photodegradation of toluene

REFERENCES

- Bari, M.A. & Kindzierski, W. B. (2018). Ambient volatile organic compounds (VOCs) in Calgary, Alberta: Sources and screening health risk assessment. *Science of The Total Environment*, 631-632, 627-640. DOI: 10.1016/j.scitotenv.2018.03.023
- Berezina E., Moiseenko K., Skorokhod A., Pankratova N. V., Belikov I., Belousov V. & Elansky N. F. (2020). Impact of VOCs and NO_x on Ozone Formation in Moscow. *Atmosphere*, 11(11), 1262. DOI: 10.3390/atmos11111262
- Binas, V., Venieri, D., Kotzias, D. & Kiriakidis, G. (2017). Modified TiO_2 based photocatalysts for improved air and health quality. *Journal of Materiomics*, 3(1), 3-16. DOI: 10.1016/j.jmat.2016.11.002
- Dinh, V. T., Thu, P. A., An, N. T., Nhan, D. N. T. & Long, N. Q. (2018). Toluene removal under humid conditions by synergistic adsorption-photocatalysis using nano TiO_2 supported on ZSM-5 synthesized from rice-husk without structuredirecting agent. *Reaction Kinetics, Mechanisms and Catalysis*, 125, 1039-1054. DOI: 10.1007/s11144-018-1452-7
- EPA (n.d.). *Volatile Organic Compound (VOC) Control Regulations*. <https://www3.epa.gov/region1/airquality/voc.html?fb>

However, when the mass percent of zeolite was decreased from 70% (TiO_2 -M60 3:7) to 80% (TiO_2 -M60 2:8), the catalytic performance was worsened. A reason for this change is that higher amount of zeolite led to lower content of TiO_2 , which resulted in a lack of active sites for the complete oxidation of toluene.

4. CONCLUSION

A series of mesoporous zeolite materials have been successfully synthesized via microwave-assisted method (MWA), which is relatively simple and timesaving compared to conventional methods. The increase in mesopores in zeolite improves the diffusion of bulky aromatics and adsorption capacity regarding the original micropore - dominant zeolite. When mesoporous zeolite was combined with TiO_2 (P25) to catalyze the photodegradation of toluene, it helped improve the photocatalytic activity and stability of the transition metal oxide. The optimal catalytic performance, which gives high toluene removal and durability, was attained from a TiO_2 -M60 mixing ratio of 3:7.

ACKNOWLEDGEMENT

We acknowledge Ho Chi Minh City University of Technology (HCMUT) and VNU-HCM for supporting this study. This research is funded by Ho Chi Minh City University of Technology (HCMUT), VNU-HCM under grant number SVKSTN-2022-KTHH-0

- clid=IwAR1FD7Ll7LdwH6LDXwIaTnPgaclx0rk2x
hnwPk17qdIGv5GxXVjGK0NiO-0
- Huang, B., Lei, C., Wei, C. & Zeng G. (2014). Chlorinated volatile organic compounds (Cl-VOCs) in environment – sources, potential human health impacts, and current remediation technologies. *Environment International*, 71, 118-138. DOI: 10.1016/j.envint.2014.06.013
- Kamal, M. S., Razzak, S. A. & Hossain, M. M. (2016). Catalytic oxidation of volatile organic compounds (VOCs) – A review. *Atmospheric Environment*, 140, 117-134. DOI: 10.1016/j.atmosenv.2016.05.031
- Kovalevskiy, N.S., Lyulyukin, M.N., Selishchev, D.S. & Kozlov, D.V. (2018). Analysis of air photocatalytic purification using a total hazard index: Effect of the composite TiO₂/zeolite photocatalyst. *Journal of Hazardous Materials*, 358, 302-309. DOI: 10.1016/j.jhazmat.2018.06.035
- Kutluay, S. & Temel, F. (2020). Silica gel based new adsorbent having enhanced VOC dynamic adsorption/desorption performance. *Colloids and Surfaces A: Physicochemical and Engineering Aspects*, 609, 125848. DOI: 10.1016/j.colsurfa.2020.125848
- Li, X., Zhang, L., Yang, Z., Wang, Yan, P., Y. & Ran, J. (2020). Adsorption materials for volatile organic compounds (VOCs) and the key factors for VOCs adsorption process: A review. *Separation and Purification Technology*, 235, 116213. DOI: 10.1016/j.seppur.2019.116213
- Mamaghani, A. H., Haghghat, F. & Lee, C. S. (2017). Photocatalytic oxidation technology for indoor environment air purification: The state-of-the-art. *Applied Catalysis B: Environmental*, 203, 247-269. DOI: 10.1016/j.apcatb.2016.10.037
- Molhave, L. (1991). Volatile Organic Compounds, Indoor Air Quality and Health. *Indoor Air*, 1(4), 357-376. DOI: 10.1111/j.1600-0668.1991.00001.x
- Mombello, D., Pira, N. L., Belforte, L., Perlo, P., Innocenti, G., Bossi, S. & Maffei, M. E. (2009). Porous anodic alumina for the adsorption of volatile organic compounds. *Sensors and Actuators B: Chemical*, 137(1), 76–82. DOI: 10.1016/j.snb.2008.11.046
- Takeuchi, M., Hidaka, M. & Anpo, M. (2012). Efficient removal of toluene and benzene in gas phase by the TiO₂/Y-zeolite hybrid photocatalyst. *Journal of Hazardous Materials*, 237-238, 133-139. DOI: 10.1016/j.jhazmat.2012.08.011
- Talaiekhazani, A., Rezania, S., Kim, K., Sanaye, R. & Amani, A. M. (2021). Recent advances in photocatalytic removal of organic and inorganic pollutants in air. *Journal of Cleaner Production*, 278, 123895. DOI: 10.1016/j.jclepro.2020.123895
- Tu, L.N.Q., Nhan, N.V.H., Dung, N. Van, An, N.T. & Long, N. Q. (2019). Enhanced photocatalytic performance and moisture tolerance of nano-sized Me/TiO₂-zeolite Y (Me = Au, Pd) for gaseous toluene removal: activity and mechanistic investigation. *Journal of Nanoparticle Research*, 21(9), 1-19. DOI: 10.1007/s11051-019-4642-y
- Zhang, F., Zhu, X., Ding, J., Qi, Z., Wang, M., Sun, S., Bao, J. & Gao, C. (2014). Mechanism study of photocatalytic degradation of gaseous toluene on TiO₂ with weak-bond adsorption analysis using in situ far infrared spectroscopy. *Catalysis Letters*, 144(6), 995–1000. DOI: 10.1007/s10562-014-1213-9